A simple kinematics to model the behavior of pressurized elbows under cyclic in-plane bending

Axel Méric, Djaffar Boussaa, Pierre Labbé, Jean-François Semblat, Pierre-Alain Nazé

Transactions of the SMiRT 27
Yokohama, Japan, March 3-8, 2024
Division II

A simple kinematics to model the behavior of pressurized elbows under cyclic in-plane bending

Axel Méric[1], Pierre Labbé[2], Djaffar Boussaa[3], Jean-François Semblat[4], Pierre-Alain Nazé[1]

[1]Geodynamique & Structure, Montrouge, France (axel.meric@geodynamique.com)
[2]IRC, ESTP Paris, Cachan, France
[3]LMA AMU CNRS Centrale (UMR7031), Marseille, France
[4]IMSIA (UMR9219), CNRS, EDF, CEA, ENSTA Paris, Institut Polytechnique de Paris, France

ABSTRACT

This paper presents a simple and efficient way to calculate the ratcheting strains at the critical locations of a pressurized elbow subjected to cycles of in-plane opening/closing. To do so, a kinematics initially proposed by Boussaa and al. *[Finite pure bending of curved pipes. 1996. Comput. Struct. 60, 1003–1012]* is presented and a way to use it in ANSYS finite element software is described. The kinematics only describes the elbow behavior when it is subjected to pure in-plane bending. The considered loading must be an history of imposed moment or elbow angle variation. Results using this kinematics are compared with experimental and numerical results of two papers from the literature. Values of ratcheting strains at critical locations of the elbow obtained with the proposed kinematics are very comparable with the ones of the literature. Moreover, computation time is divided by around 200 when using this kinematics over a shell finite element model.

INTRODUCTION

Experimental campaigns, such as the one reported and analysed in Ranganath et al. (1994), NRC (2008), Ravikiran et al. (2015), MECOS (2021), aimed to assess the piping systems strength. The studied type of loadings were seismic loadings. It has been shown that the main failure mode is by propagation of a crack at the flank of the most damaged elbow in the piping system. This is due to low-cycle fatigue damage aggravated by accumulated plastic strain resulting from high level of internal pressure. This failure mode is called fatigue-ratcheting. Moreover, the main response mode of elbow is, most of the time, the one that tends to open or close the elbow. Thus, it is of interest to determine the state of strain of a pressurized elbow where ratcheting occurs to assess its fatigue life.

Three main ways to model an elbow are conceivable (Attia et al., 2022). The option of enriched beam type elements based on Von Kármán (1911) has been explored by Bathe and Almeida (1980, 1982) and by Yan and Jospin (1999). The cross-sectional deformation modes such as ovalization are described by Fourier series. The use of shell elements, based on Kirchoff-Love (1888) theory or Reissner-Mindlin (Reissner, 1945; Mindlin, 1951) for respectively thin and thick shells, can be used to model thin to thick pressurized elbow. Three dimensional elements remain the more accurate choice to calculate accurately the state of stress/strain in the elbow thickness, at the cost of computation time. In the literature, to study the strain field evolution of pressurized elbows, where ratcheting occurs, 2D shell elements (Hassan and Rahman, 2009; Ravikiran et al. 2015; Islam and Hassan, 2019) and 3D solid elements (Chatzopoulou and Karamanos, 2021) are often used.

This study puts forward a simple and different kinematics to determine the states of strain and stress in a pressurized pipe elbow submitted to a load history of opening/closing bending moment or rotation. The goal is to minimize the time of calculation that can be important for this kind of problem where elbows are often modelled by 3D solid or 2D shell finite elements.

First, we present the kinematics initially proposed by Boussaa (1992) and Boussaa et al. (1996) to model the elbow behavior under in-plane pure bending. The studied elbow section is chosen

the farthest away from the straight parts, as it seems to be the most vulnerable section. This kinematics implies that the structure can be modelled by considering an axisymmetric kinematics plus an additional degree of freedom which represents the elbow angle variation. Secondly, a procedure is proposed to use this kinematics into ANSYS (2020) thanks to generalized plane strain elements. A way to define the history of angle variation that is imposed to the elbow is presented. This history can be the result of a static or a transient analysis. The method proposed in this study is compared with a numerical study on the ratcheting circumferential strain at an elbow flank carried out by Ravikiran et al. (2015). It is also compared with a numerical and experimental study performed by Islam and Hassan (2019) on the ratcheting strains evolution at different location of an elbow cross-section.

KINEMATICS

The kinematics considered in this study has been thoroughly studied in Boussaa (1992) and in Boussaa et al (1996). The pressurized elbow is considered to be a part of a torus, which means it is idealized as a three-dimensional body with axisymmetric properties: the cross-section geometry is supposed to be invariant with respect to the rotation around Z axis of the elbow. This initial configuration is represented in figure 1.

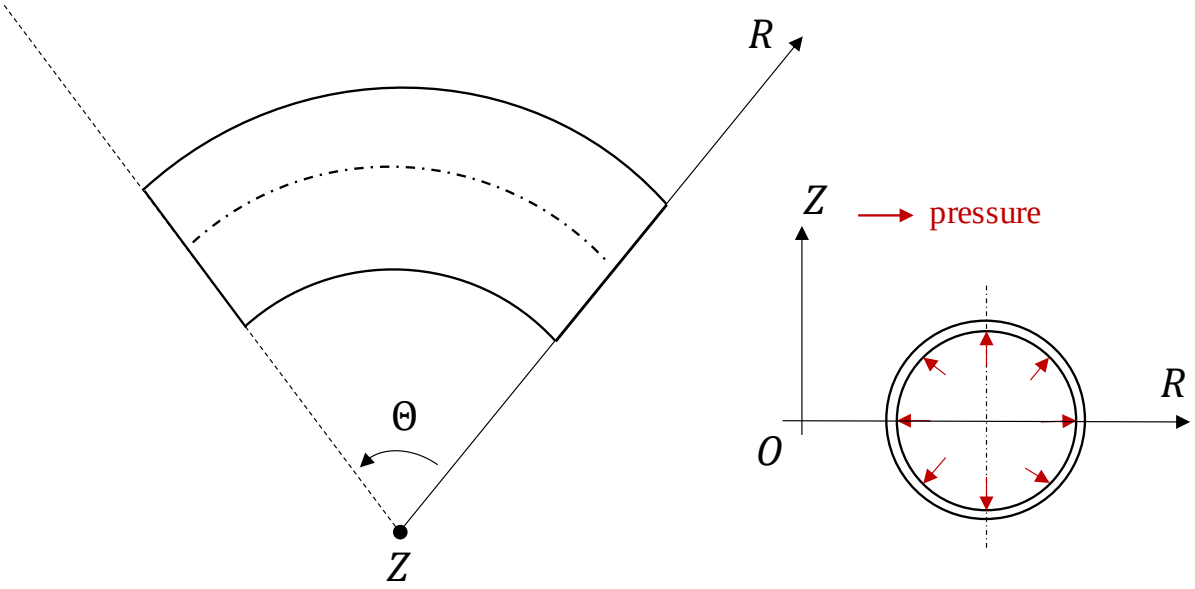

Figure 1: The elbow: configuration of study

In this initial configuration, we denote M the position of a particle of the elbow. This position is expressed according to the cylindrical coordinates (R,Θ,Z) and the unit vectors $(\underline{E_R},\underline{E_\Theta},\underline{E_Z})$ as:

$$M = O + R\underline{E_R} + Z\underline{E_Z} \tag{1}$$

When the elbow is subjected to an external load, it is deformed and the particle of initial position M is at the position m in the deformed configuration. This new position is represented by the coordinates (r,θ,z) and the unit vectors $(\underline{e_r},\underline{e_\theta},\underline{e_z})$ and expressed as:

$$m = O + r\underline{e_r} + z\underline{e_z} \tag{2}$$

The following hypothesis is made regarding this geometrical evolution:

$$\begin{cases} r = r(R, Z, t) \\ \theta = \big(1 + a(t)\big)\Theta \\ z = z(R, Z, t) \end{cases} \tag{3}$$

In the above, $a(t)$ is a scalar representing the elbow angle variation. Indeed, by denoting θ_0 the elbow angle at a time t_0 and θ_1 the elbow angle at time t_1 after deformation as represented in figure 2, we can calculate $a(t)$ according to equations 3:

$$a(t_1) = \frac{\theta_1 - \theta_0}{\theta_0} = \frac{\Delta\theta}{\theta_0} \tag{4}$$

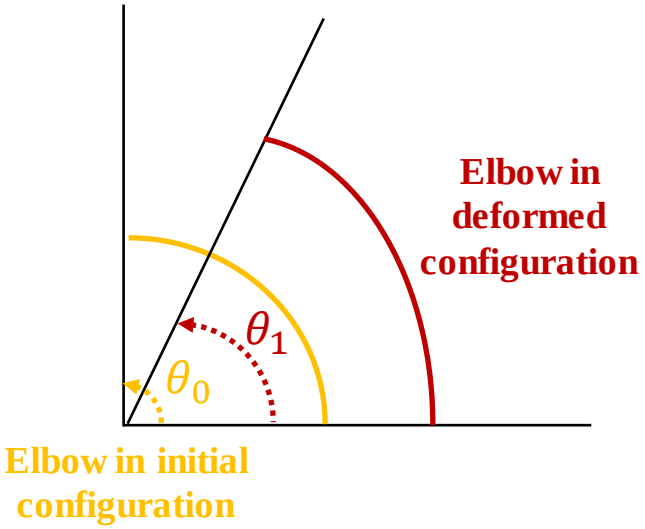

Figure 2: Initial and deformed configuration of an elbow

The parameter $a(t)$ represents both the solution or the imposed loading of the mechanical problem. This choice of kinematics implies the following consequences:

- Usual hypothesis of Navier-Bernoulli is still respected. Plane sections remain plane, the section normal vector remains normal.
- The kinematics only represents the elbow behavior under in-plane pure bending. Out of plane bending or more complex loadings cannot be represented. Nonetheless, the main response of elbows under dynamic loadings is the excessive opening/closing that induce the elbow failure by fatigue ratcheting. This has been observed, for example, in EPRI experimental campaigns by Ranganath et al. (1994).
- There is the possibility to add the pressure as a loading.
- The elbow remains an elbow in the sense that it is still a three-dimensional body represented by a section rotating around the same axis.
- The problem can be decomposed into an axisymmetric problem with an added degree of freedom. Indeed, by fixing $a(t) = 0$ in equations (3), the kinematics of a three-dimensional axisymmetric problem is obtained.
- No hypotheses were made regarding the cross-section geometry. This implies that different kind of elbow can be modelled, thin or thick elbows, elbows with elliptic sections or with variation of thickness in the section.
- As r and z are independent of Θ, it implies that all cross sections deform in the same way. Thus, it is only necessary to model one cross section.

The last consequence is important regarding the computation time. The proposed kinematics represents the three-dimensional behavior of the elbow when it is subjected to in-plane pure-bending as a three-dimensional solid element finite element model would do, but computation time should be much faster.

This kinematics can be represented by generalized plane strain (GPS) finite elements which are plane strain elements where the fibre length is assumed to be finite. Thus, fibre direction stresses or strains are not fixed at zero. These elements are programmed in ANSYS (2020) finite element software under a key option of the PLANE182 and PLANE183 elements (four and eight nodes plane elements respectively). The elbow is modelled and meshed by representing the section in the X-Y plane. A starting point is given by the user and an ending point is defined by defining the elbow angle and fibre length as represented in figure 3. The distance of the cross-section centre to the X-Y plane origin defines the radius of curvature. Boundary conditions can be applied on the cross-section and on the ending point. Hereunder are listed the boundary conditions that can be applied to the ending point:

- Applied force or displacement in the fibre length direction;
- Moment or rotation around the X axis;
- Moment or rotation around the Y axis.

In the case of an elbow, if the radius of curvature is defined along the X axis, the rotation axis of the elbow should be the Y axis, and the moment or rotation should be applied around the Y axis too. The imposed rotation corresponds to $\Delta\theta$ of equation 4. Internal pressure can be applied through surface loads.

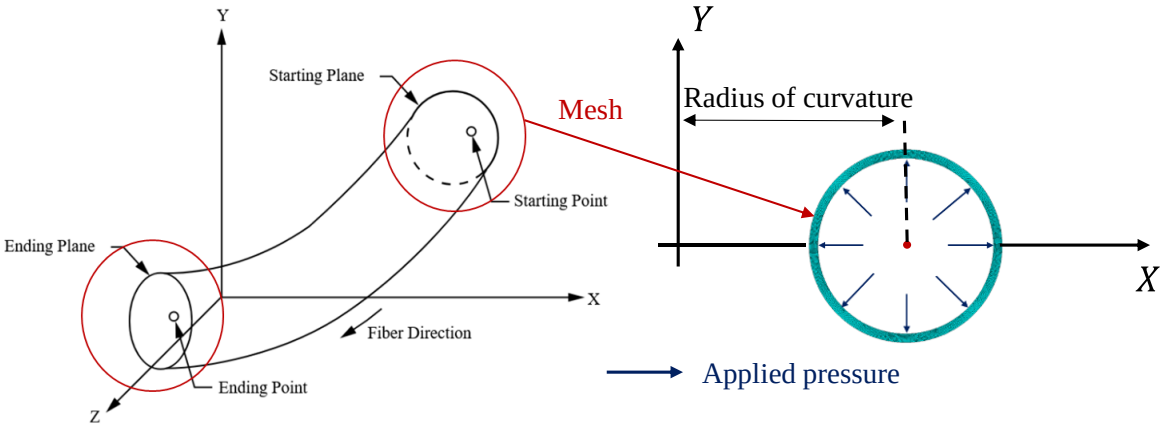

Figure 3: Generalized plane strain model, ANSYS (2020)

To avoid rigid body motions, imposed displacement in the fibre length should be imposed at the ending point and, in the case of figure 3 where the radius of curvature is defined along the X axis, Y displacement of one point (one fibre) of the mesh should be imposed.

Next sections present comparisons between results obtained with the presented kinematics and numerical results of Ravikiran et al. (2015) and of Islam and Hassan (2019).

THE BARC NUMERICAL CALCULATIONS

The Indian Bhabha Atomic Research Centre (BARC) has recently performed an experimental campaign to assess the strength of piping systems subjected to dynamic seismic loads. Components and systems were studied. The case of the ratcheting of an elbow under imposed displacement of opening/closing is considered here. The results are taken from Ravikiran et al. (2015).

A 90° elbow is considered. Its radius of curvature is 228.6mm, its outer diameter is 168.3mm and its thickness 7mm. The ends of the elbow are attached to straight pipes whose length is equal to three times the outer diameter of the elbow in order to take into account the straight parts stiffening effect. The finite element model of Ravikiran et al. is represented in figure 4. The elbow is meshed by shell elements, one end of the elbow is embedded and a static displacement is imposed at the other end of the elbow. Moment, rotation, and circumferential strain are calculated with this model. The material constitutive relationship considered is the Chaboche (1991) elasto-plastic model. The parameters are defined in Ravikiran et al. (2015).

The imposed displacement is represented in figure 5. To compare Ravikiran et al. (2015) results and our proposed generalized plane strain kinematics results, it its necessary to convert this imposed displacement history into an elbow angle variation history. To do so, a finite element model composed of 175 elbow elements (Elbow290 elements in ANSYS) is made. These elements are based on the works of Bathe and Almeida (1980, 1982) and of Yan and Jospin (1999). This model is represented in figure 4. Geometric non-linearities are activated. The elbow angle variation is obtained by studying a 1° small portion of the elbow centre, far away from the straight parts to diminish their effect. The value of $\Delta\theta$ of equation 4 is obtained this way and is represented in figure 5. This is input loading of the GPS kinematics. Since we obtained $\Delta\theta$ by studying an elbow portion of 1°, the curved pipe studied with the GPS kinematics should be a 1° elbow to coincide with the previously obtained $\Delta\theta$ history. By doing so, the value of $a(t)$ from equation 4 is provided correctly into the model. The mesh of the GPS kinematics is represented in figure 6. It is composed of 5500 PLANE183 elements so that there are 9 elements in the thickness.

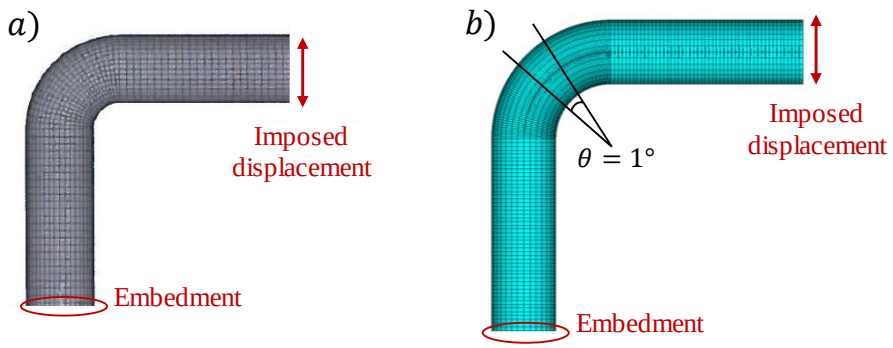

Figure 4: Finite elements model – a): Ravikiran et al. (2015) shell model – b): Elbow290 model

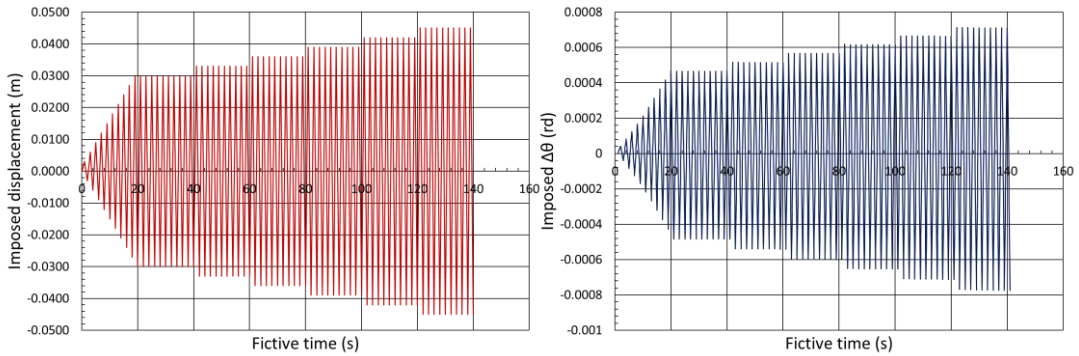

Figure 5: Imposed displacement and imposed elbow angle variation

Fibre length displacement at the ending point and the Y displacement of one node of the mesh are set to zero to avoid rigid body motion.

The elbow is also pressurized at $P = 12\ MPa$. This value was chosen in Ravikiran et al. (2015) to produce a hoop stress of value $\sigma_{\theta\theta} = 140\ MPa$ in the elbow under pressure only. However, this value of hoop stress is calculated according to the straight pipes under internal pressure formula. It is recalled in (11):

$$\sigma_{\theta\theta}(r) = P\frac{r_i^2}{r_o^2 - r_i^2}\left(1 + \frac{r_o^2}{r^2}\right) \tag{11}$$

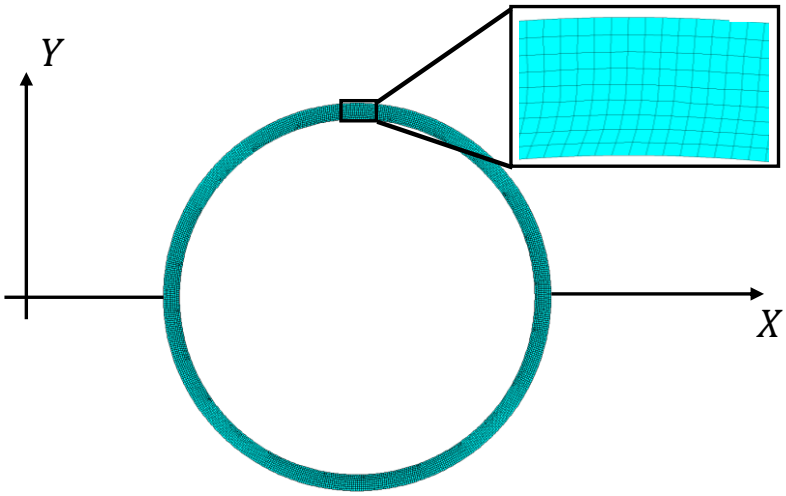

Figure 6: GPS kinematics mesh

Where r_0 and r_i are the outer and inner radius respectively. In the case of an elbow under pressure, there is no reason that the scalar $a(t)$ from equation 3 is equal to zero when the elbow is pressurized. Thus, it is possible that the elbow is opened or closed when it is pressurized. It is represented in figure 7 which represents the GPS kinematics result when elbow is only pressurized. Maximum hoop stress value is located at the intrados and is equal to $\sigma_{\theta\theta} = 185\ MPa$ which is higher than the one predicted by (11).

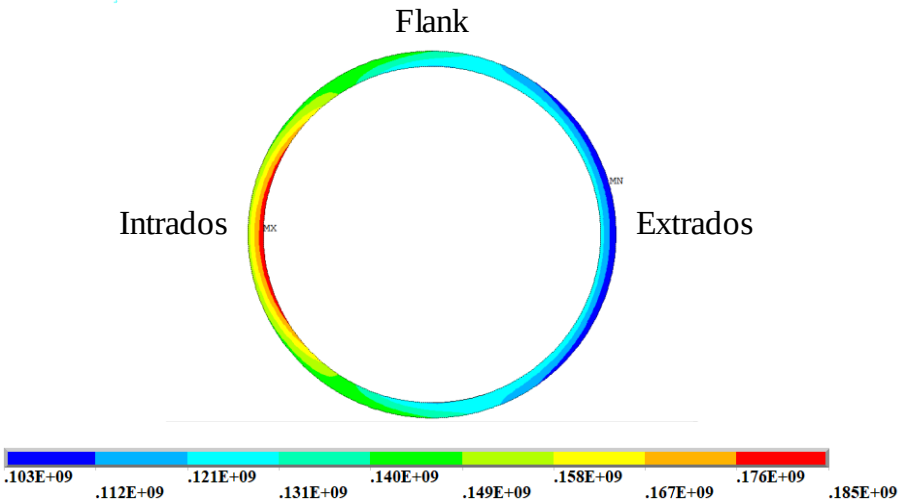

Figure 7: Elbow under internal pressure – Hoop Stress (in Pa)

The $\Delta\theta$ loading history described in figure 5 is applied to the GPS model after the initiation of pressure. The time step is equal to 0.005s. To capture the elbow asymmetric behavior, geometric non-linearities are taken into account. Results of moment-rotation curves and moment-hoop strain curves are presented in figures 8 and 9. Results of moment-hoop strain curves are compared with the one of the BARC (Ravikiran et al., 2015). As shown in figure 8, The GPS kinematics represent the asymmetric behavior of the elbow. The more the elbow is opened, the harder it is to open it. On the contrary, the more the elbow is closed, the easier it is to close it. This due to the ovalization of the cross section as it has been discussed by Von Karman (1911), Brazier (1927), Clark and Reissner (1951). Moment-hoop strain curves represented in figure 9 are obtained for a hoop strain measured at the outer skin of the elbow flank. Regarding hoop strain values, the results of the GPS model are in good accordance with the one obtained by Ravikiran et al. (2015). Both maximum absolute value of the hoop strain at the end of the loading are around 6.2%. A difference regarding the moment-hoop strain loops should be noted, as values of moment at closure are higher for the BARC results. This is possibly due to the straight parts effect that are not considered in the GPS kinematics or to the choice of shell elements. Straight parts tend to stiffen the elbow by preventing ovalization. Values of moment at opening are in good accordance.

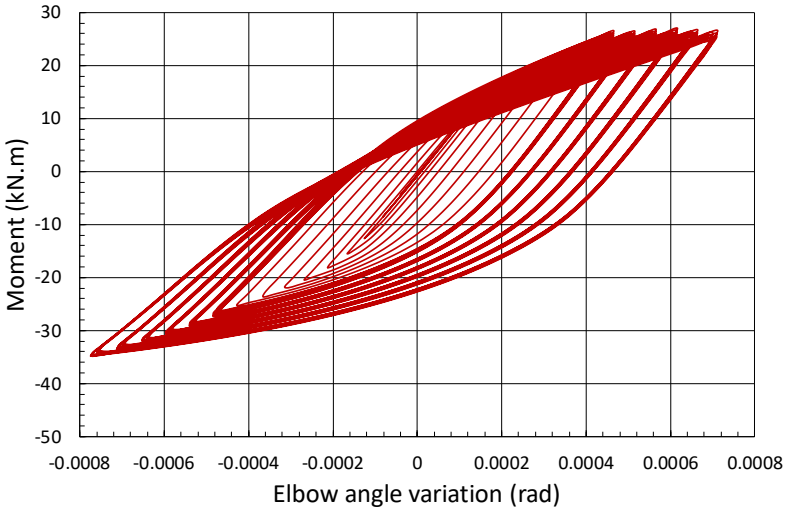

Figure 8: Moment rotation curves

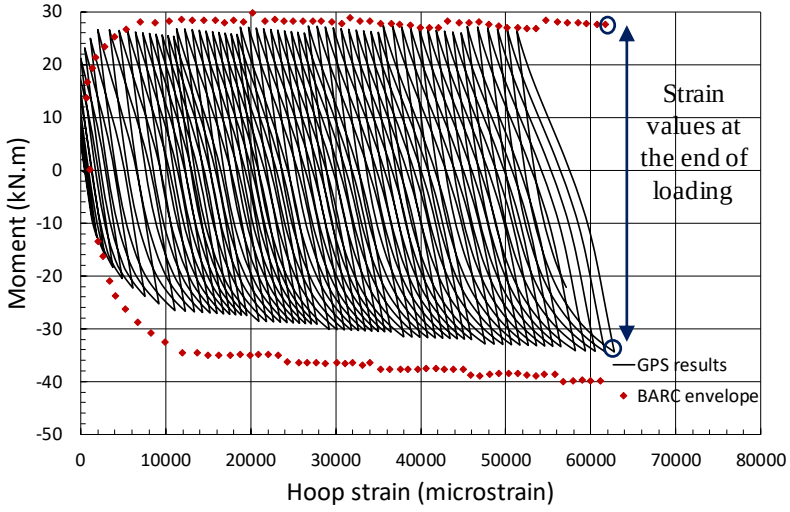

Figure 9: Moment hoop strain curves – Comparison between GPS results and BARC results (Ravikiran et al., 2015)

Regarding the computation time, a comparison has been made between the GPS model and a reproduced Ravikiran et al. (2015) shell finite element model on just a few cycles. The computation time is divided by around 200 when using the GPS model. This deviation should be much more important if the GPS model computation time would be compared with the one of a model made of 3D solid elements.

THE ISLAM AND HASSAN (2019) EXPERIMENTAL AND NUMERICAL RESULTS

This section aims to compare the results obtained by Islam and Hassan (2019) in terms of the state of strain of a long radius elbow. They obtained experimental and numerical results on several geometries of elbows. The one that is considered in this paper is a 3.75mm thick stainless-steel elbow. Its external diameter is 60.56mm, the radius of curvature is 75mm. The constitutive model for the steel used by these authors is the Chaboche (1991) elasto-plastic model with a Voce (1955) model for the non-linear isotropic hardening. Four sets of parameters are considered for the Chaboche model (Islam and Hassan, 2019). The elbow is pressurized at 11.8 MPa and subjected to cycles of in-plane opening and closing imposed displacement as shown in figure 10. The displacement is imposed during 200 cycles of amplitudes 11.8mm (1 fictive second corresponds to half a cycle in this study). Strains are measured at three locations: at the intrados, the extrados and the flank of the most critical elbow section. The same procedure as described in the previous section is applied to predict the state of strain with the GPS model. A finite element model with enriched beam elements is used (see figure 10) to obtain the angle variation $\Delta\theta$ of a 1° angle portion of the elbow under consideration. The history of $\Delta\theta$ is then applied in the GPS model.

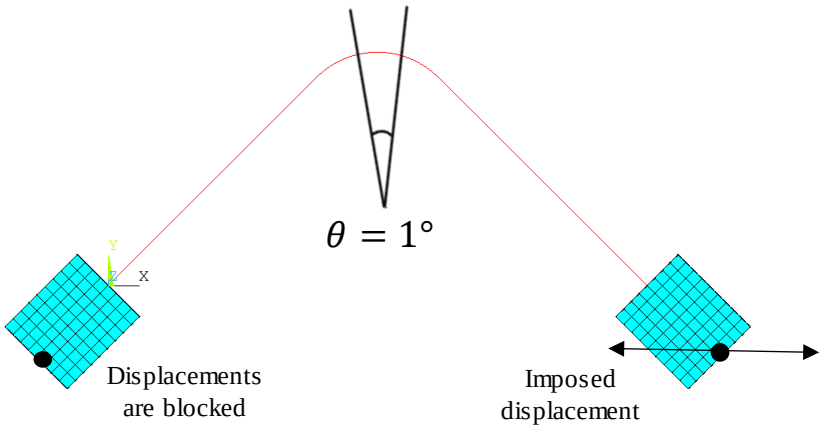

Figure 10: Islam and Hassan (2019) considered elbow.

Results of total strains are presented in figure 11. Hoop strain is measured at the flank and the extrados. Axial strain is measured at the intrados. The results of the GPS model are presented and compared with the mean strain experimental and numerical results of Islam and Hassan (2019). Their numerical results were obtained with a shell finite element model. Results of Hoop strain at flank location show a good accordance between experimental results and GPS results. Indeed, no plastic shakedown is predicted after 100 cycles whereas the Islam and Hassan numerical results predict a shakedown after 50 cycles. Mean values are very close. This result highlights that strain results are not only dependant on the material constitutive relationship but also on the choice of kinematics (solid vs shell modelling). Regarding the axial strain at intrados, the experimental mean strain values are not correctly predicted by either the GPS model or Islam and Hassan shell finite element model. However, the GPS model results are closer to the experimental results than the shell finite element model. It predicts a plastic shakedown at around the same number of cycles whereas the shell model does not predict accommodation after 200 cycles. Results of hoop strain at extrados are not well predicted by the GPS model as no plastic shakedown can be observed yet. Nonetheless, the sign of the strain is correctly obtained whereas the shell model gives a negative sign for the strain. As it is not discussed here, the

choice of the material constitutive relationship also plays an important role on the strain results (Islam and Hassan, 2019) and can explain some of the differences between the experimental and numerical results. However, better results were obtained with the GPS model overall.

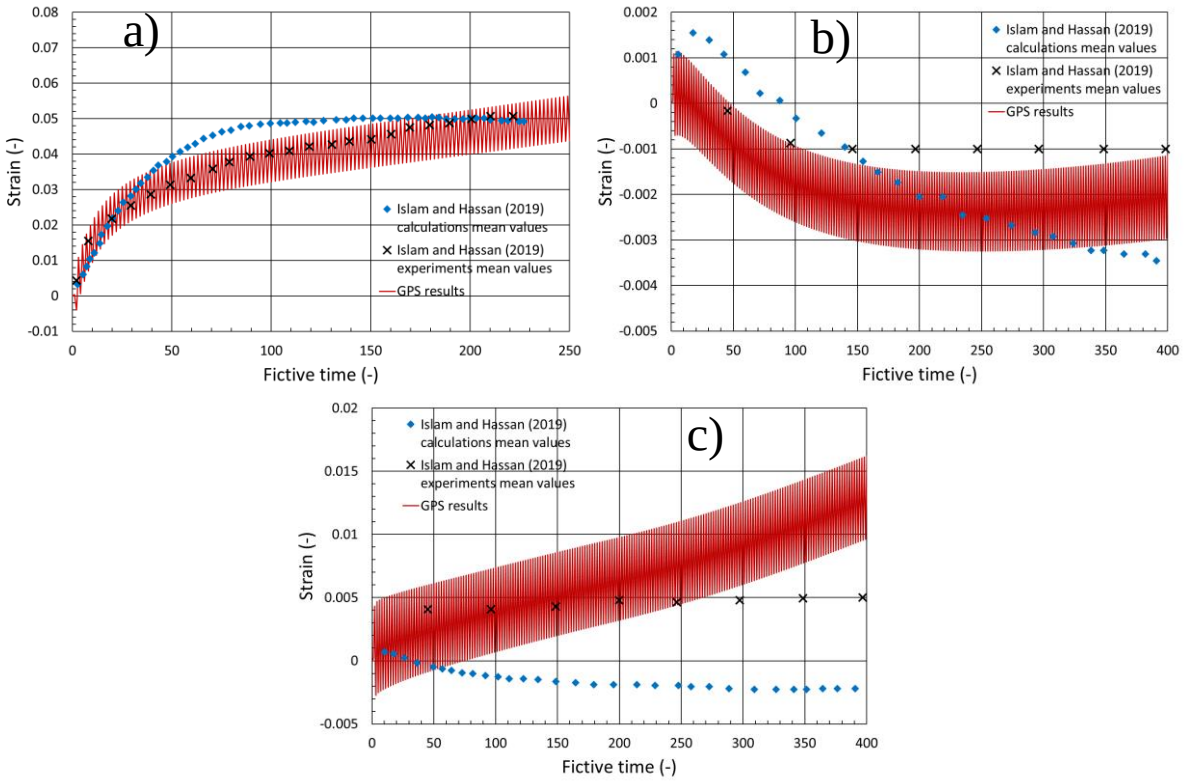

Figure 11: Comparison of GPS with Islam and Hassan (2019) strain results at different locations – a) Hoop strain at flank location – b) Axial strain at intrados – c) Hoop strain at extrados.

CONCLUSION

A simple kinematics initially proposed by Boussaa (1992) and Boussaa et al. (1996) has been used to calculate the ratcheting strains of pressurized elbows under cyclic loadings. This kinematics can be represented by generalized plane strain (GPS) finite elements available in ANSYS (2020). It enables the study of the behavior of the pressurized elbow under pure in-plane bending. The imposed loading must either be a history of moment or elbow angle variation. This history can be obtained from a beam/pipe finite element model. Then, accurate results of ratcheting strains can be obtained at the elbow critical locations.

The GPS model has been compared with numerical results from (Ravikiran et al., 2015). Hoop strain at the outer skin of the elbow flank was well predicted. It was also tested against the experimental and numerical results of Islam and Hassan (2019). These comparisons showed that not only the material constitutive relationship plays a role in the ratcheting strain calculation but the kinematics also. The results of hoop strain at elbow flank location obtained from the GPS model were in good accordance with the experimental results. The computation time was divided by around 200 using the GPS model.

The efficient computation time of the GPS model is promising in the goal to avoid making 3D solid of 2D shell finite element models to assess the state of strain in the most damaged elbow of a piping system at the end of cyclic loading such as an earthquake. The combination of pipe plus GPS finite elements models should maybe be considered instead.

REFERENCES

Ansys® (2020). *Academic Research Mechanical, Release* 20.1.

Attia, S., Mohareb, M., Martens, M., Ghodsi, N.Y., Li, Y., Adeeb, S. (2022). *Shell finite element formulation for geometrically nonlinear analysis of curved thin-walled pipes*. Thin Walled Struct. 173, 108971.

Bathe, K.J., Almeida, C.A. (1982). *A Simple and Effective Pipe Elbow Element—Interaction Effects*. J. Appl. Mech. 49, 165–171.

Bathe, K.J., Almeida, C.A. (1980). *A Simple and Effective Pipe Elbow Element—Linear Analysis*. J. Appl. Mech. 47, 93–100.

Boussaa, D., Van, K.D., Labbé, P., Tang, H.T. (1996). *Finite pure bending of curved pipes*. Comput. Struct. 60, 1003–1012.

Boussaa, D. (1992). *Flexion plane du tuyau coudé et endommagement sous séisme*. PhD, L'école nationale des ponts et chaussées.

Brazier, L. G. (1927). *On the flexure of thin cylindrical shells and other "thin" sections*. Proc. R. Soc. Lond. Ser. Contain. Pap. Math. Phys. Character 116, 104–114.

Chaboche, J.L. (1991). *On some modifications of kinematic hardening to improve the description of ratchetting effects*. Int. J. Plast. 7.

Chatzopoulou, G., Karamanos, S.A. (2021*). Numerical implementation of bounding-surface model for simulating cyclic inelastic response of metal piping components*. Finite Elem. Anal. Des. 185, 103493.

Clark, R. A., Reissner, E. (1951). *Bending of curved tubes. Massachusetts Institute of Technology*. Cambridge, Advances in Applied Mechanics, Volume 2, Pages 93-122.

Hassan, T., Rahman, S.M. (2009). *Simulation of Ratcheting Responses of Elbow Piping Components*, in: Volume 1: Codes and Standards. Presented at the ASME 2009 Pressure Vessels and Piping Conference, ASMEDC, Prague, Czech Republic, pp. 103–108.

Islam, N., Hassan, T. (2019). *Development of a novel constitutive model for improved structural integrity analysis of piping components*. Int. J. Press. Vessels Pip. 177, 103989.

Kármán, T. von (1911). *Uber den Mechanismus der Widerstander den ein bewegter Körper in einer Flüsseigkeit afahrt. Gott. Nachr*, 509–517.

Love, A. E. H. (1888). *The small free vibrations and deformation of a thin elastic shell*. Philos. Trans. R. Soc. London, Ser. A 179 (Jan): 491-546.

MECOS GE (2021). *Towards New Approach for Seismic Design of Piping systems*, Final Report, endorsed for publishing by seismic subgroup of Working Group on Integrity and Ageing of Components and Structures (IAGE, WG), Nuclear Energy Agency Committee on the Safety of Nuclear Installations.

Mindlin, RD. (1951). *Influence of rotatory inertia and shear in flexural motion of isotropic, elastic plates*. ASME Journal of Applied Mechanics.

NRC, U.S. (2008). *Seismic Analysis of Large-Scale Piping Systems for the JNES-NUPEC Ultimate Strength Piping Test Program*. United States Nuclear Regulatory Commission. NUREG/CR-6983, BNL-NUREG-81548-2008.

Ranganath, S. (1994). *Piping and Fitting Dynamic Reliability Program*. EPRI TR-102792. Paolo Alta, CA.

Ravikiran, A., Dubey, P. N., Agrawal, M. K., Reddy, G. R. (2018). *Experimental and numerical studies of ratcheting in pressurized stainless steel piping systems under seismic load*, BARC/2015/E/018.

Reissner, E. (1945). *The effect of transverse shear deformation on the bending of elastic plates*. J. Appl. Mech. Jun 1945, 12(2): A69-A77.

Voce, E. (1955). *Metallurgica*. Col. 51, 219.

Yan, A.M., Jospin, R.J., Nguyen, D.H. (1999). *An enhanced pipe elbow element - Application in plastic limit analysis of pipe structures*. Int. J. Numer. Methods Eng. 46, 409–431.